Investigative Microgravity Deployment Tests of the Canisterized Satellite Dispenser (CSD)

Stephen K. Tullino[1]
Air Force Research Laboratory Space Vehicles Directorate, Small Satellite Portfolio, Kirtland AFB, NM, 87120

Eric D. Swenson[2]
Harris Corporation Space and Intelligence Systems, Palm Bay, FL, 87120

Jessica L. Marshall Tullino[3]
Alumna, Georgia Institute of Technology Aerospace Systems Design Laboratory, Atlanta, GA, 30332

Planetary Systems Corporation (PSC) developed the Canisterized Satellite Dispenser (CSD) to provide a more secure, predictable, and consistent deployment system for CubeSats. Though the CSD has proven its safety and reliability on orbit and in other air- and ground-based tests, there is still not enough data required to develop analytical profiles describing CSD deployment linear and angular deployment velocities and accelerations. In response, researchers at AFIT conducted lab-based experiments to characterize CSD deployment dynamics with the objective of creating and tuning a predictive model simulation in 2017. A result of this research, the researchers decided to test the CSD further in microgravity conditions to further improve data quality. AFRL led tests were conducted at NASA Glenn Research Center's microgravity drop tower with the assistance of AFIT and NASA researchers in attempt to collect sufficient data in a relevant environment to enhance characterization of the CSD for risk reduction and mission planning.

Nomenclature

$t_{\alpha/2}$	=	t Statistic (two-tailed)
α	=	Level of Significance
$\bar{x}$	=	Sample Mean
s	=	Sample Standard Deviation
n	=	Sample Size

I. Introduction

THE CubeSat was first developed in 1999 at California Polytechnic State University (Cal Poly) to enable academia to explore space and achieve various scientific objectives. CubeSats are measured in units of "U," where 1U is a 10 cm^3 cube (1L in volume) having a maximum mass of 1.33 kg. CubeSats vary in size, but they are generally found in 1U, 2U, 3U, 6U, and 12U variants. (1) They require a separate dispensing device as most launch vehicles only accommodate a main payload, and most CubeSats typically share a ride on these launches. Most CubeSat dispensers, such as Cal Poly's Pico-satellite Orbital Deployer (P-Pod) and the Innovative Solutions in Space (ISIS) ISIPOD, eject payloads via push-plates attached to large coil springs. Despite its robustness, a coil spring applies non-uniform force to the push-plate and can unevenly transfer forces out of line with the CubeSat's center of mass. This results in a torque action which can introduce an initial tipoff spin during CubeSat deployment. (1) The P-POD and ISIPOD deployers use four guide rails that require extremely tight tolerance gaps (<0.1 mm for the P-POD) to constrain the

[1] Deputy Program Manager, Small Satellite Portfolio, Member AIAA.
[2] Mission Solutions Business Area Chief Technologist, Senior Member AIAA.
[3] M.S. Alumna, Department of Aerospace Engineering, Member AIAA.

CubeSat which can result in unpredictable vibrational loads during transportation and launch. Misalignment can result in the CubeSat becoming lodged in the deployer and thus fails to deploy. (1) Another limitation of these is that their coil springs are governed by Hooke's Law, where the force provided by a compressed spring is proportional to the compressed distance, resulting in a deployment force that decreases linearly. (1) As CubeSats have sophisticated, the need to provide an equally refined dispenser has become critical to achieving mission objectives. To address this, Planetary Systems Corporation (PSC) created the CSD to use of one (or more) constant-force springs (i.e. wound steel bands, like the ones found in a tape measure), and provide a predictable uniform dispensing force as they do not obey Hooke's Law. The CSD (specifically the 3U variant) met TRL9 on its inaugural launch on 29 Sep 2013, and since then several (including 6U variants) have flown since. (2) (3) Instead of using the "traditional" P-POD/ISIPOD guide rails, PSC uses two guide rails. A CSD CubeSat chassis has a base plate with two tabs running along the chassis sides, and interface with the guide rails during ejection. (1) The guide rails clamp down on the payload tabs when the CSD door is closed. This tab-clamping preloading of the payload to the CSD a stiff invariant load, which allows accurate dynamic modeling to predict responses from vibratory testing and space flight. (2)

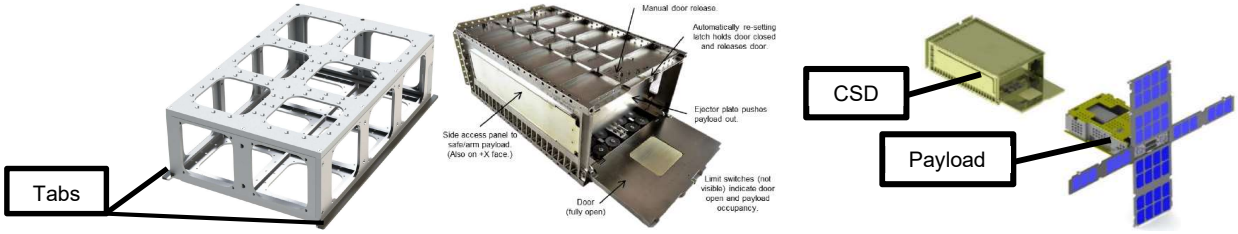

Figures 1, 2, 3. CSD CubeSat Chassis with Tabs (left), 6U CSD (center), and CSD with CubeSat (right) *(2) (4)*

A. Background

In 2014, PSC conducted four days of deployment tests on a NASA C-9 "Vomit Comet" in order to measure rotation rates and velocities of 3U and 6U payloads as they eject from a CSD in a simulated zero-g environment. The objective of the test was to uncover failure modes and performance deficiencies as CubeSats have an average on-orbit failure rate of approximately 50% due to failure to reach orbit, inability to control, no contact, etc. (5) PSC researchers found that the CSD dispenses payloads with lower rotation rates than other dispensers at a difference of 1-2 orders of magnitude. Unfortunately, PSC also noted multiple sources of error. The main source of error was that the C-9 induces rates of rotation (~6°/s). These initial induced rates caused by the C-9 produced higher measured angular rates after dispensing, as seen in Fig 4. PSC suspects that error was also introduced into the data by IMU bias and drift, resulting in notable error in ejection velocity calculations, as well as due to their test setup, specifically that the frame used to secure the CSD was not stiff enough. This was evident when transients were produced when the CSD door sprang open. Using the C-9 required time for tuning and acclimation (i.e. getting used to the flight profile of the C-9) which resulted in 24 missed dispensing opportunities. Given this issue, multiple flight campaigns would be necessary to attain the desired data. However, at a cost of $400K+ per flight this would not be financially feasible. (5)

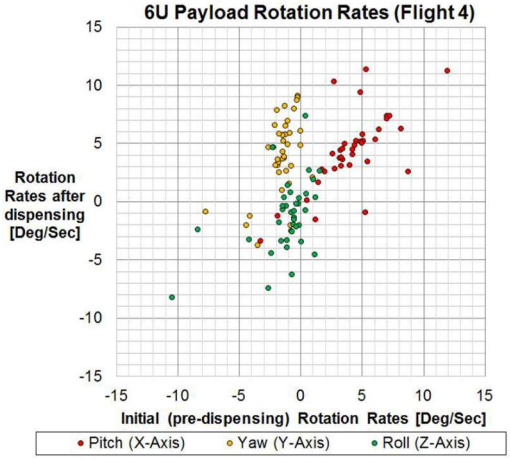

Figure 4. 6U CubeSat Payload Rotation Rates Coupled with Rotation from C-9 (5)

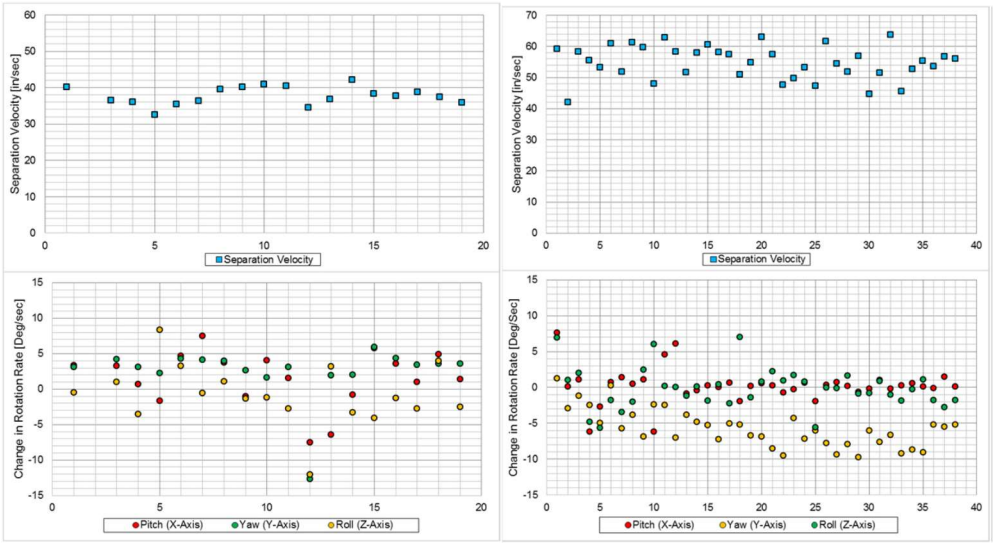

Figures 5, 6. 3U (left) and 6U (right) Separation Velocities and Rotation rates (2)

As seen in Figs. 5-6, PSC was still able to gather sufficient information to develop preliminary linear ejection profiles, as seen in Fig. 7. Because the angular rate data covered a wide range of values, the best way for PSC to characterize rotation tip-offs was to select the worst-case rate seen on any axis, which was around 10°/s. (2) (6)

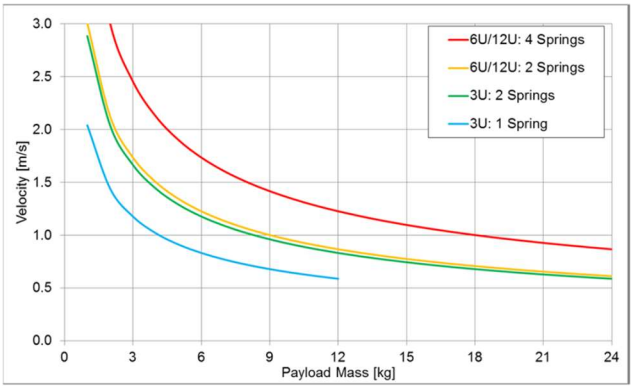

Figure 7. PSC Payload Ejection Velocity (2)

AFIT researchers deemed it necessary to continue to explore the ejection properties of the CSD (specifically the 2-spring 6U version) in order to develop a higher fidelity analytical model and further understanding factors that affect the deployment of a CubeSat. To do this, the following tests were conducted as part of S. Tullino's master's thesis research effort (23): static push plate force tests, horizontal CSD ejection tests with a payload-mounted accelerometer which was subsequently repeated with an IMU, characterization of rail friction, door interference characterization via accelerometers and high-speed cameras, and vertical deployments to characterize push plate feet contacts. An analytical MATLAB simulation was created from this data based on these CSD measurements and specifications. The primary limitation of these experiments was gravity, as the CSD is designed to operate in micro gravity. Gravitational impacts included cantilevered motion of the payload as it deployed horizontally, resulting in much higher levels of friction imparted on the rails, which is much higher in the horizontal as opposed to the vertical deployment tests. Only light payloads (i.e. a CubeSat base plate at 0.70 kg was used) could successfully be ejected from the CSD because a full chassis often got stuck in the guide rails. Initial data yielded irregular motion which prompted an investigation with high speed cameras. The door was observed to oscillate during release, interfered with and contacted the base plate during ejection. After isolating the door, data was cleaner, and yielded an average base plate deployment acceleration of 14.25 m/s2, with a standard deviation of 5.55 m/s^2. The acceleration data yielded velocity and displacement profiles better fit MATLAB predictions. Moreover, the final linear velocity of 3.25 m/s, reasonably agreed with PSC's profile (reasonably because PSC doesn't plot payloads that low in mass in Fig. 7). The corresponding gyroscopic data yielded the locations on when and where tipoff moments were applied to the payload

(after 0.319 m of payload deployment travel), as well as when the payload left the confines of the CSD guide rail (after 0.338 m of travel). Though much was learned, gravity still prevented a more "realistic" test deployment of a CubeSat, which led to the need to conduct microgravity tests to collect more realistic data to validate PSC's initial findings.

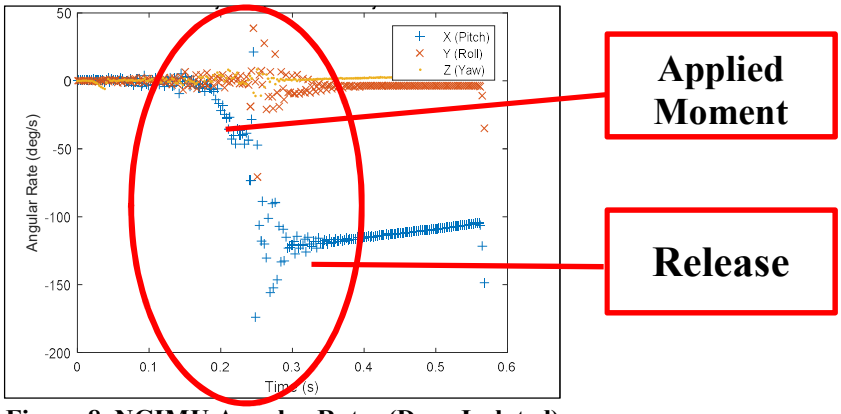

Figure 8. NGIMU Angular Rates (Door Isolated)

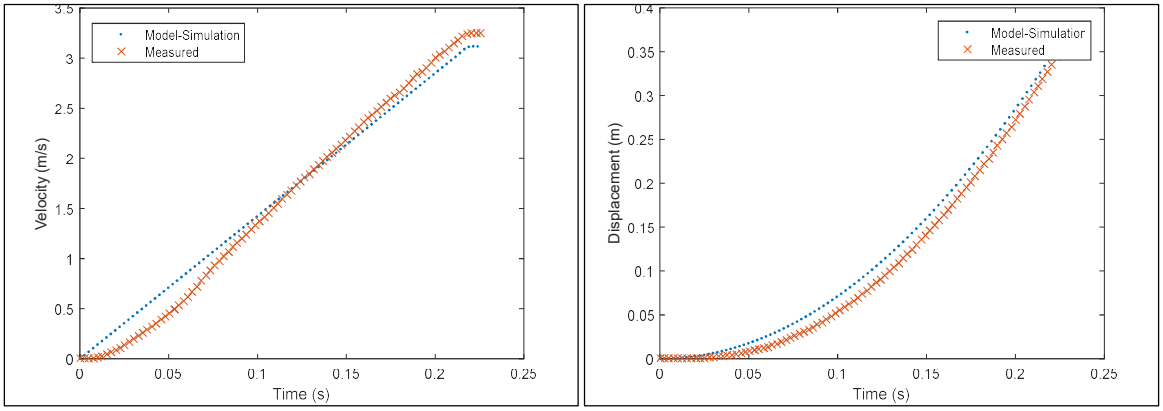

Figures 9, 10. Integrated NGIMU Data vs Model: Velocity (left) and Displacement (right) (Door Isolated)

CSD deploys CubeSats via a spring-loaded push plate which transfers its ejection force to the payload through contact points on the backside of the payload. PSC requires that there be at least three contact points with the push plate centered on the payload's center of mass. (7) A recent test by AFIT on the Pumpkin SUPERNOVA CubeSat chassis inspired the investigation of how important the location of these feet are with respect to tipoff rates. The CubeSat chassis underwent random vibration testing in the 6U CSD and after the test, uneven wear-marks were identified on the CSD push plate, implying uneven contact with the push plate. Theoretically, an imbalance in push plate feet contact, or the feet not centered on the center of mass, a moment about the center of mass can be induced during ejection. (7) To test this concept, a 3-D 6U chassis was printed and reduced in mass to make it light as possible, yet maintaining a full chassis shape.

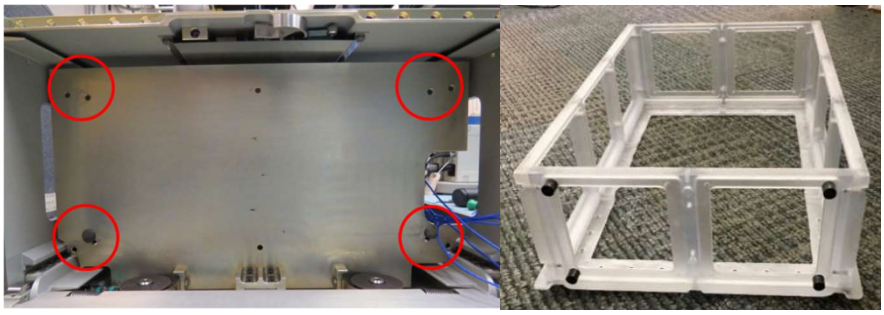

Figures 11, 12. Wear Marks from Pumpkin SUPERNOVA Vibration Test Demonstrating Uneven Contact (left) (8) **and 3-D Printed 6U Chassis with Contact Feet (right)**

Using the original 7.89 N push plate force value, it was necessary to test with a payload lighter than 0.8 kg to allow the CSD ejection acceleration from the pusher plate to exceed the acceleration due to gravity. This is important to prevent gravity from inducing any angular rates, the 3-D printed chassis had to be deployed vertically upwards. The 3-D printed chassis had contact feet attached to its backside in order to test the effects the feet have on a deploying payload. These force distribution tests will test a range of scenarios in order to develop a profile characterizing the effects of uneven force distribution being applied to the payload. From this push plate feet contact experiment, it was apparent that the model needs further tuning with respect to tip-off rates caused by the push plate feet, where there were instances when the model was off by ~50°/s on an axis. This was realized because the multiple instances of IMU data were consistent in performance and had small standard deviations amongst each other. It was suspected that the deviations between theoretical and measured values were due to the analytical model not accounting for perturbations in the push plate. Moreover, the model most likely deviated from measured values because the parameters used may not have been precise enough. This led to the realization that microgravity testing was necessary to validate flight data to overcome the aforementioned barriers posed by gravity.

B. Motivation

AFIT's desire to further refine these ejection profiles was motivated by the fact that the Space and Naval Warfare Systems Command (SPAWAR) is planning on conducting 20 missions using the Pumpkin SUPERNOVA spacecraft bus, which requires the use of the CSD. NASA has also purchased 13 CSDs for secondary payloads (from government, international, academic, and independent mission partners) on the maiden flight of the Space Launch System, Exploration Mission 1 (EM-1). (6) CSDs will be attached to SLS' Multi-Purpose Crew Vehicle (MPCV) Stage Adaptor (MSA) and each CSD will eject its designated payload through the Orion Stage Adaptor. (9)

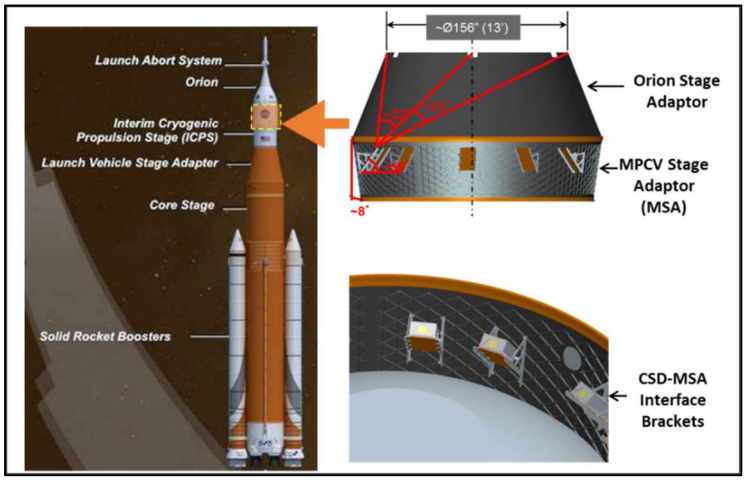

Figure 13. CSD Location on SLS. *Stage adaptor location (left). Installation and orientation of the CSD, along with expected flight path (right). (9)*

To ensure the safety of both the SLS and secondary payloads, NASA has mandated that each CubeSat payload have a 4ft (1.219m) diameter ejection clearance zone "bubble." A potential concern is that as a payload passes through the Orion Stage Adaptor, it only has ~2.5ft (0.762m) of clearance between it and the lip of the vehicle. (9)

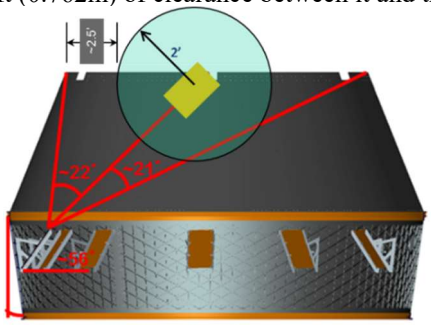

Figure 14. Payload "Bubble" Clearance Zone *(9)*

A significant risk associated with this configuration is that excessive CubeSat tumbling could increase the chance of impacting with the vehicle, which could result in collateral damage. This fact in itself is justification for the need to further refine the mapping of the CSD's ejection profile. NASA's Secondary Payload team has agreed that better understanding of how the CSD deploys would aid payload developers in both their hardware design and attitude control system setup, mission planning, as well as in mission concept of operations (CONOPS). (9) Another item to note is that in order to simplify the development of the 13 secondary payloads, NASA has recommended that these CubeSats not use the standard contact points enveloping the spacecraft's center of mass. (PSC specifications recommend that a CubeSat have at least three contact points.) (7) For example, the Pumpkin SUPERNOVA brand of chassis uses four contact feet to envelope the center of mass.

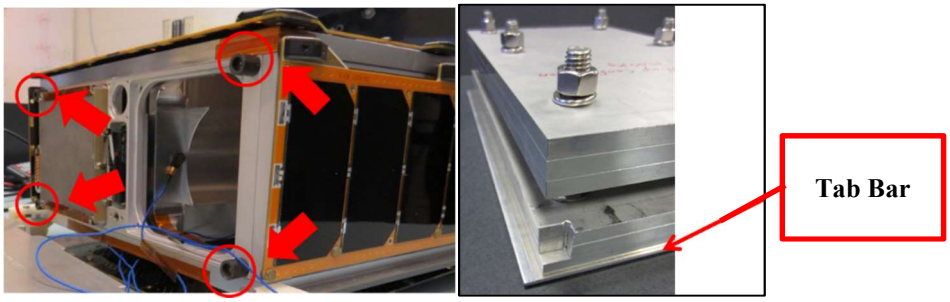

Figures 15, 16. Contact Feet on SUPERNOVA 6U CubeSat Chassis (left) (10) **and NASA Experimental Test Mass with Tab Bar** (9) **(right)**

The contact point specification is intended to limit any tipoff moments applied to the spacecraft during ejection. NASA has proposed in 2016 instead of this configuration that payloads only contact the CSD push plate by the bottom tabs normally found in CSD payloads (or in this case, an even further simplification by not machining leaving a rear "tab" extended to protrude on the rear face in order to provide a full contact bar (Fig 16.). The risk of this design simplification is the probability of having an increased moment along the horizontal axis upon ejection. Unless the center of mass is near the CubeSat chassis base plate, the applied force will be offset from the center of mass (assuming the center of mass is within the 80 x 60 mm^2 window around the geometric center per PSC's 6U payload spec), which will induce a significant moment (7). A benefit of this setup is that it does reduce moments along the vertical axis, which allows mission planners to primarily focus on counteracting only one induced moment upon deployment. It is good to note that as of 2018, NASA has updated its guidance where three separation switches are required, and payload designers are encouraged to envelope the center of mass, per PSC spec. (11)

C. Drop Tower Selection

From lessons learned from challenges during AFIT bench tests, it was verified that the conducting of deployment tests in a microgravity environment is ideal because the CSD is designed to function in microgravity. For the needs of the experiment, NASA's drop towers were selected because they provided an economical microgravity environment with an adequate volume to conduct the experiment in. At NASA Glenn Research Center's drop tower facility in Cleveland, OH, two drop towers were available to choose from:

1) 5.18 s Duration Drop Tower – 132 m (432 ft) drop (12)
    a. ~$8k/day (without including labor and preparation costs)
    b. Allows up to 2-3 drops/day due to it having vacuum chamber properties (requires air being pumped out for each test)

2) 2.2 s Duration Drop Tower – 24 m (17 ft) drop (13)
    a. ~$2k/day (without including labor and preparation costs)
    b. Allows up to 12-15 drops/day since there is no vacuum chamber. A drag shield is used instead to reduce air drag effects on freefalling payloads (discussed later)

Simulations were conducted in MATLAB to determine the range of times required to fully eject a payload, and these were seen to have a duration between 0.2–1.4 s, which is below the maximum 2.2 s. Because of this, the 2.2s drop tower was selected. The experiment chassis for the drop tower has a size envelope of 38 inches wide, 15.75 inches deep, and a height of either 33 inches, or 42.63 inches when using an extended drag shield spacer. (13) (14)\For a spacecraft chassis to be ejected out of a CSD vertically downwards, clear the CSD door, and travel at least one chassis length before stopping, 35 inches is required for a testing envelope (found from the end-to-end combined length of a CSD, the CSD door opening radius, and a spacecraft chassis). This fits right into the 2.2 s drop tower experimental chassis with the extended 42.63 inches height drag shield configuration. It doesn't matter that the CSD points downwards versus horizontally because since the apparatus is in freefall.

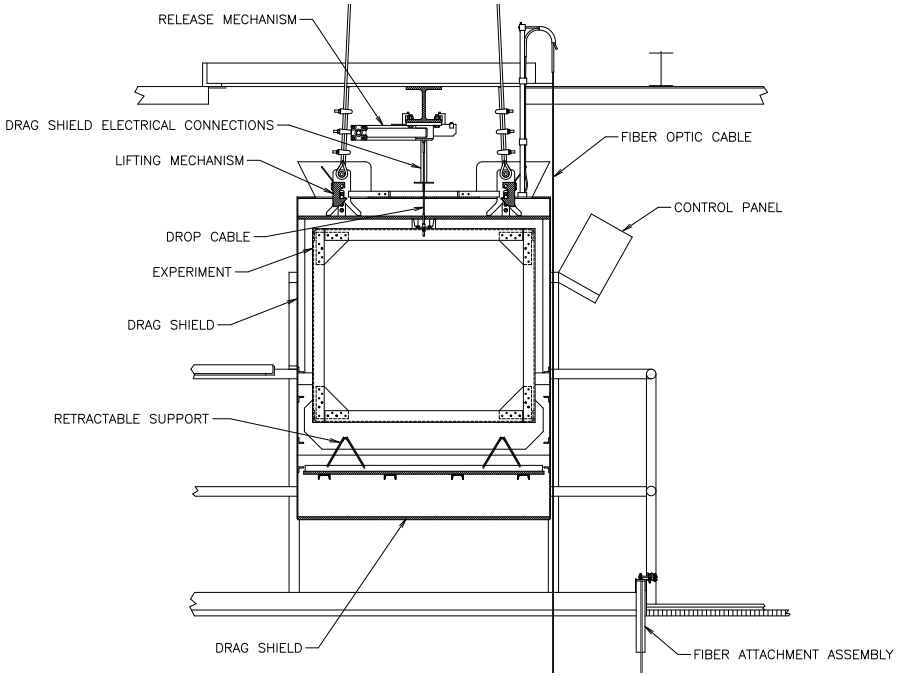

Figure 17. Tower Experiment Setup (14)

As shown in Fig. 17, the experiment experiment sits within a drop tower experimental test frame, which is then placed in a larger drag shield. Both the drag shield and inner frame are suspended and dropped. An air bag at the bottom of the tower safely stops the experiment's freefall. The drag shield protects the inner experiment frame from air drag where the shield slows down and the inner frame has the freedom to independently "float" freely in freefall (microgravity) within the larger envelope of the drag shield. Because the extended height drag shield is ideal to maximize the experiment's operational envelope, a custom inner frame was created in order to ensure the CSD is properly attached with flexible configuration options.

D. Research Objectives

- The primary objective of this research is to validate and clarify PSC's previous microgravity test data in order to enhance the confidence in CSD ejection performance characterization for a nominal payload within CSD spec. Nominal spec is defined as a payload with a center of mass within an 80mm square centered on the rear face of the spacecraft contacting the push plate, and at least three push plate contact points enveloping the spacecraft COM. For our case, the four-contact point configuration seen on the Pumpkin SUPERNOVA (a common CubeSat spacecraft) will be used.
- The second objective is to evaluate the spacecraft configuration being encouraged by NASA for use on the SLS EM-1 mission, where instead of the prescribed three minimum push plate contact points, the push plate would only push on the bottom tabs of the spacecraft.

- A third objective is to explore the effects of deviating from PSC COM spec when it comes to COM location. This is accomplished by shifting the COM to a top-heavy configuration not enveloped by the push plate contacts. The NASA tab-only configuration is also considered for this objective.
- A fourth objective is to evaluate the impact that Moog isolators have on ejection motion. With PSC's assistance, Moog has provided this experiment eight of their motion isolators that are to be used with each CSD that will be on EM-1 (i.e. each CSD will be connected to eight isolators when interfacing with the SLS rocket). These are designed to reduce the effect of vibrations felt by the respective CubeSat during launch.
- An optional objective (time permitting) is to explore the effects of removing a push plate contact point, thus ceasing to envelope the COM.

II. Methodology

A. Experiment Data

The linear acceleration and rotation rates of the CubeSat chassis exiting the CSD were measured by an integrated inertial measurement unit (IMU) that has MEMS accelerometers to capture linear accelerations and a microelectromechanical system (MEMS) gyroscope that captures angular rates. The IMU must be standalone where it is self-powered and capable of saving its own data. The IMU that met these requirements was the high-performance Next Generation IMU (NGIMU), made by X-Io Technologies.

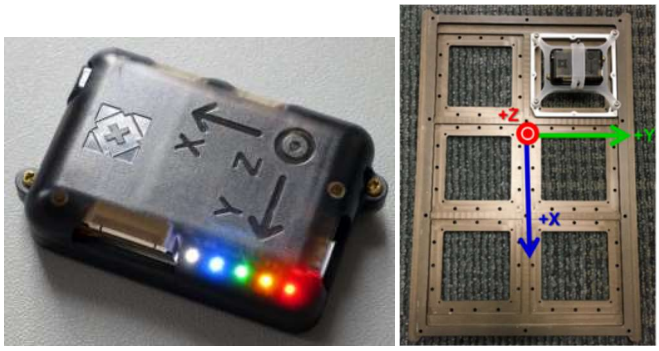

Figures 18, 19. X-Io NGIMU (right) (15) **and mounted NGIMU w/ Coordinate System (left)**

The NGIMU allows users to set frequency/sampling rate of its gyroscope and accelerometer, as well as utilize many other features, such as magnetometers, temperature sensors, and it even has a motion-activated setting. For the sake of practicality, the NGIMU used during the microgravity tests were set to a sampling rate of 400 Hz for both gyroscopic and accelerometer sensors, which have data acquisition ranges of +/-2000°/s and +/- 16g, respectively. Gyroscopic accuracy resolution is 0.06°/s, and the accelerometer has an accuracy resolution of 490 µg.

B. Sources of Variation

The controlled regressors used during the test were:

- The variation of push-plate contact points, specifically:
  - Four contact feet fully engaging the CSD push-plate, enveloping the center of mass (COM) per CSD spec. The use of four contact points was to mimic the Pumpkin SUPERNOVA, a popular CSD satellite bus that inspired previous CSD research. (16) (17)
  - No contact feet used, where only the spacecraft tabs were contacting the CSD push-plate. This was the original NASA SLS EM-1 configuration, and though no longer recommended, it is still worth demonstrating this configuration's effects for those payload planners still considering its use.
  - Three contact feet used, again using the SUPERNOVA setup, in order to demonstrate potential effects of failing to successfully envelope the spacecraft COM per spec.

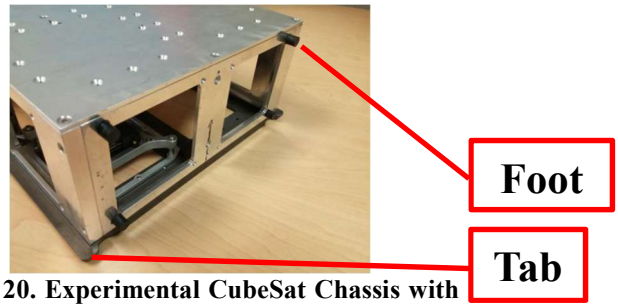

Figure 20. Experimental CubeSat Chassis with four (4) contact feet. *Note tabs on the bottom.*

- The varying of center of mass (and subsequently moment of inertia) to demonstrate the effects of spacecraft mass properties not within CSD spec. Two configurations were used in the tests: nominal/centered COM within the prescribed CSD COM location envelope, and top-heavy COM that is not within specs.

Figures 21, 22, 23. Centered COM Mass Stack Setup (left), Top-Heavy COM Mass Stack Setup (center), Mass Stacks in Chassis (right). *Note CubeSat chassis top is removed for easier visualization.*

  - Corresponding mass specs are shown in Figs. 18 thru 20 for the centered configuration

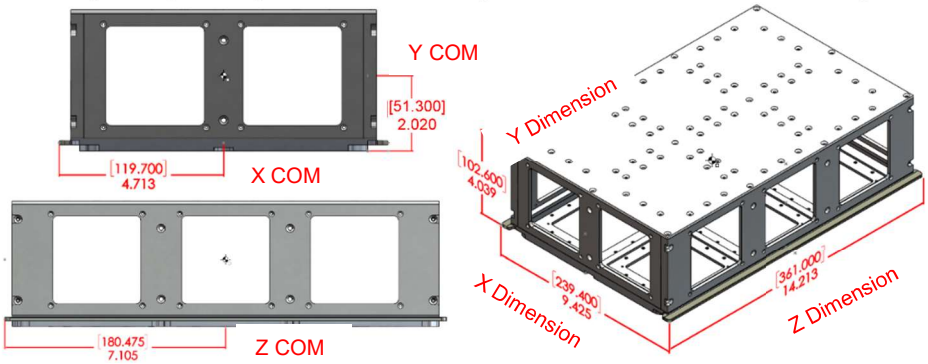

Figures 24, 25, 26. COM for Centered Configuration: Z-Face with X and Y COM Coordinates (top left), X Face with Z COM Coordinate (bottom left), ISO View with CubeSat Chassis Dimensions. *For the high COM configuration, only difference is that the Y COM location is at 67.400mm instead*

  - Centered: mass = 5.57 kg, I_{xx} = 37897.2 kg-mm^2, I_{yy} =56089.4 kg-mm^2, I_{zz} = 30017.2 kg-mm^2
  - Top heavy: mass = 5.88 kg, I_{xx} = 38387.2 kg-mm^2, I_{yy} =58970.7 kg-mm^2, I_{zz} = 31454.1 kg-mm^2

- Using of Moog isolators with the CSD to evaluate how it effects linear acceleration and tip-off angular rates.

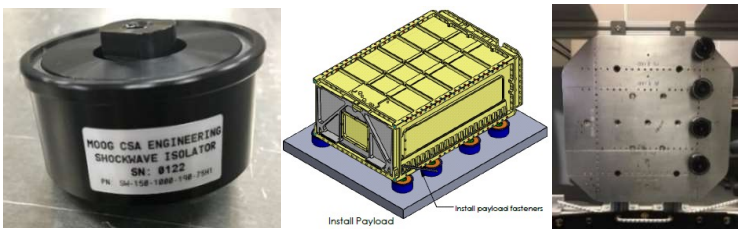

Figures 27, 28, and 29. Moog Isolator (left), Moog CAD Drawing of CSD Attached to Isolators (center) (18)**, Isolator Attached to Experiment Chassis Mounting Plate (right)**

Potential nuisance sources of variation would be flexion of the CSD push plate, and the spacecraft not being fully seated in the CSD against the push plate, both of which would yield uneven deployment forces being applied to the spacecraft. Ignorable variation sources would be air resistance because the spacecraft is travelling ~1m, half of which is within the CSD. "Wind" induced by falling in the drop tower is negligible because of the apparatus' drag shield.

C. Drop Tower Setup

As discussed earlier, it was decided that opting for the extended drag shield would be preferable, as it enabled sufficient distance for a CubeSat chassis to fly out of a CSD, completely clear the deployer, and provide the necessary flight time (<0.5s) to accurately capture tipoff rates and ejection velocity data. Using NASA specs, the AFIT team built an experiment chassis with an 80/20 aluminum frame, with 0.25in aluminum plates to protect the CSD and NASA drag shield. (With respect to the 2.2s drop tower, designs have been advised to be designed to withstand 30g's when impacting the air bag, however data has shown a maximum impulse of 23g.) (13) (19) A hook-and-loop lined catcher bag is affixed at the bottom of the experiment chassis. The hook-and-loop arrests the CubeSat (also covered with hook-and-loop tape) when it hits the bag, and protects the CubeSat and chassis from damage during air bag impact.

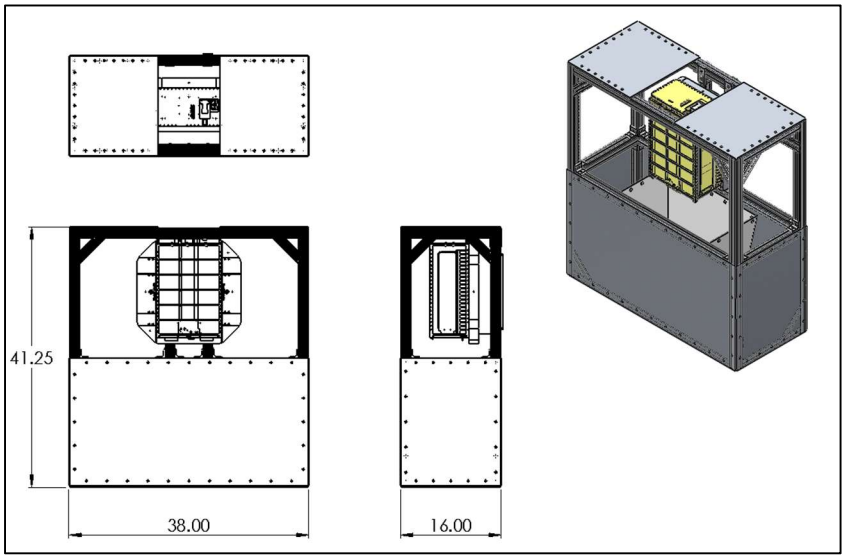

Figure 30. AFIT Drop Tower Experiment Chassis Design *(20) Dimensions are in inches.*

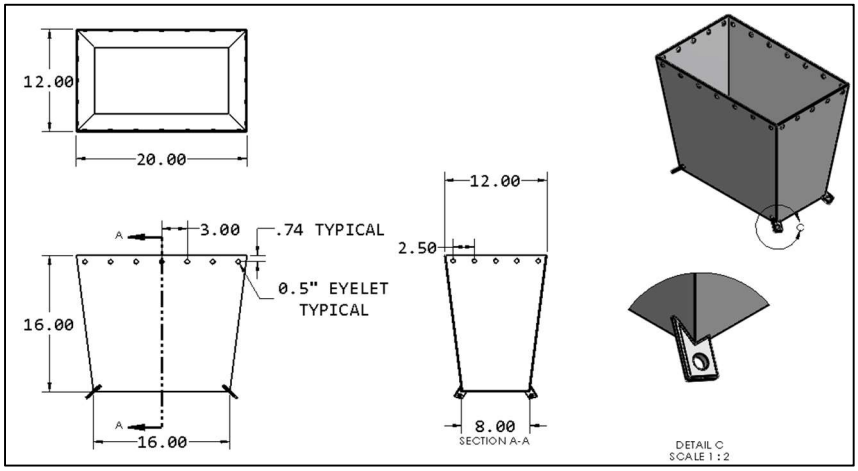

Figure 31. AFIT Drop Tower Chassis Catcher Bag. *The bag is made of vinyl-coated nylon tarpaulin often used on semi-trucks. It is attached to the rig chassis, suspended, and held open with elastic cords via 0.5in grommets. Lining the bag is industrial hook-and-loop fastening material, which arrests the CubeSat chassis.*

Figure 32. Assembled CubeSat Chassis with Hook and Loop Tape

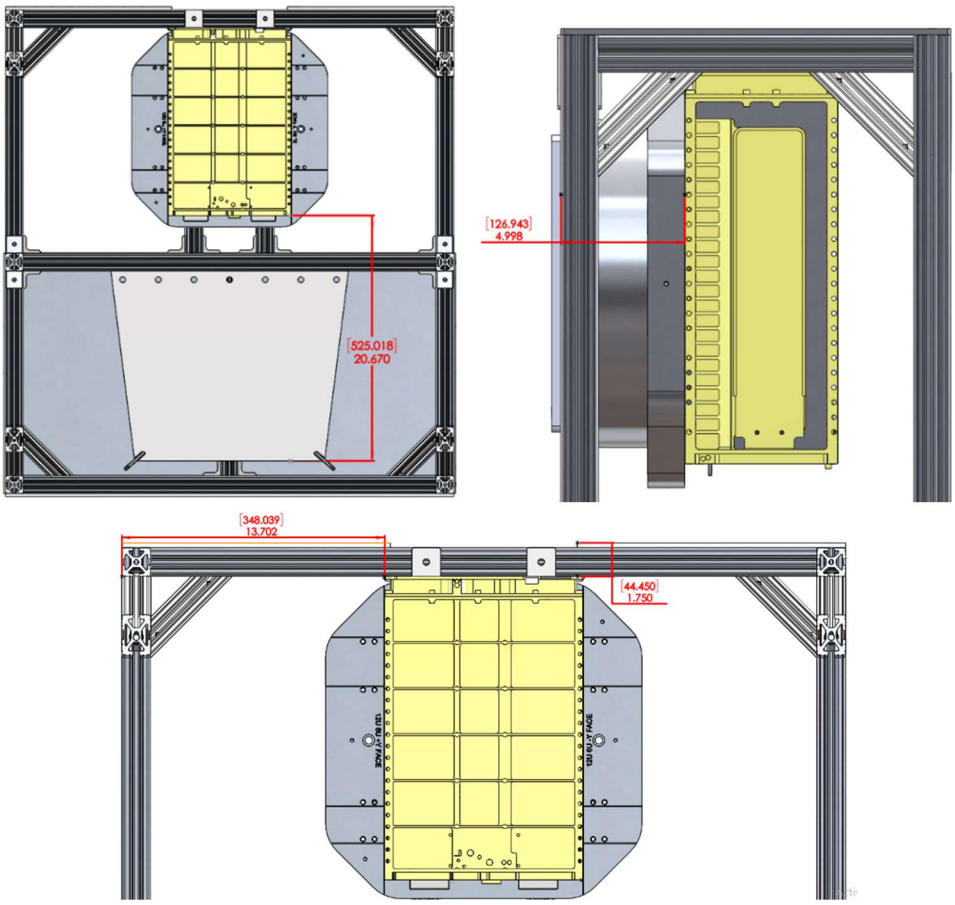

Figures 33 (top left), 34 (top right), and 35 (bottom). CSD Placement in AFIT Drop Tower Chassis.

The CSD is mounted to the rig via directly to an aluminum plate (Figs. 33-35), or via Moog isolators (Figs. 27-29). All CSD access panels have been removed by this point. The CSD is connected to a special trigger mechanism, which triggers off of a monitor circuit. The Trigger connects to banana plugs on the drag shield electrical connections (Figs. 36-38), and deploys the CSD in 0.2s when the drop tower experimental rig and drag shield fall, disconnecting the banana plugs, thus opening the monitor circuit.

Figures 36, 37, and 38. Trigger Settings (left), Trigger connections (Center), Trigger CSD Connection (right)

NASA GRC technicians then attach special lighting and high speed camera fixtures in order to monitor and record the experiment during flight. Moreover, NASA GRC technicians add ballast to the rig to ensure the experimental rig COM is in the geometric center in order to ensure the rig doesn't veer off course while in freefall. Experimental rig setup is shown and annotated in Fig. 39.

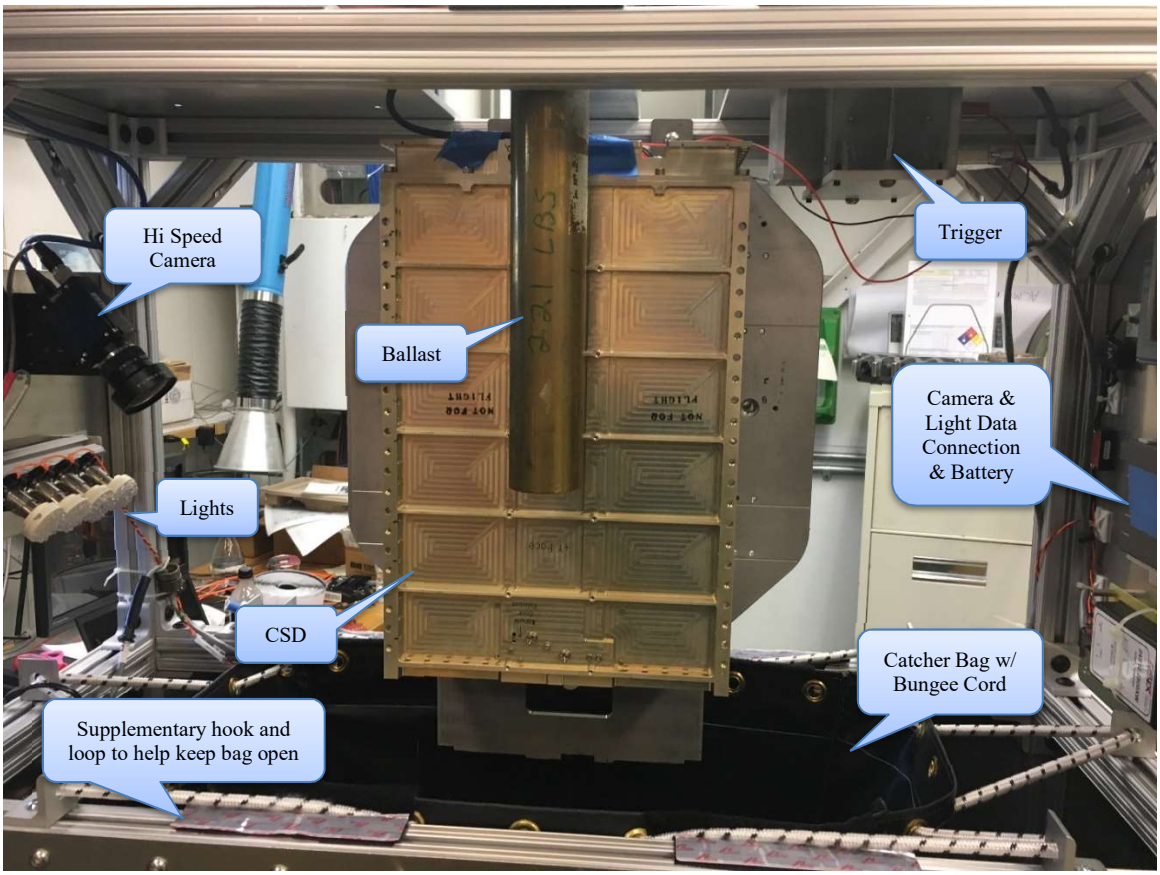

Figure 39. Experimental Rig Setup

When the experimental rig was ready at the prep floor, the CubeSat chassis was configured, all bolts were torqued to spec, and hook and loop tape was adhered to the CubeSat, as required. Prior to insertion into the CSD, the NGIMU was checked, and the CubeSat chassis was inserted into the CSD and locked. The experimental rig was hoisted into the bottom portion of the drag shield, and then encapsulated by the top portion of the drag shield. When the drag shield was secured, the rig was hoisted to the top of the drop tower. At the top of the drop tower, drag shield electrical connections were made, the drag shield access doors were opened to do final drag shield preps, and the NGIMU was manually turned on. The access doors were shut, and the experiment was released. The experiment was hoisted back to the prep floor, where the experiment rig was reset. During reset, the NGIMU is manually turned off, and data was extracted from it onto the experimenter's laptop.

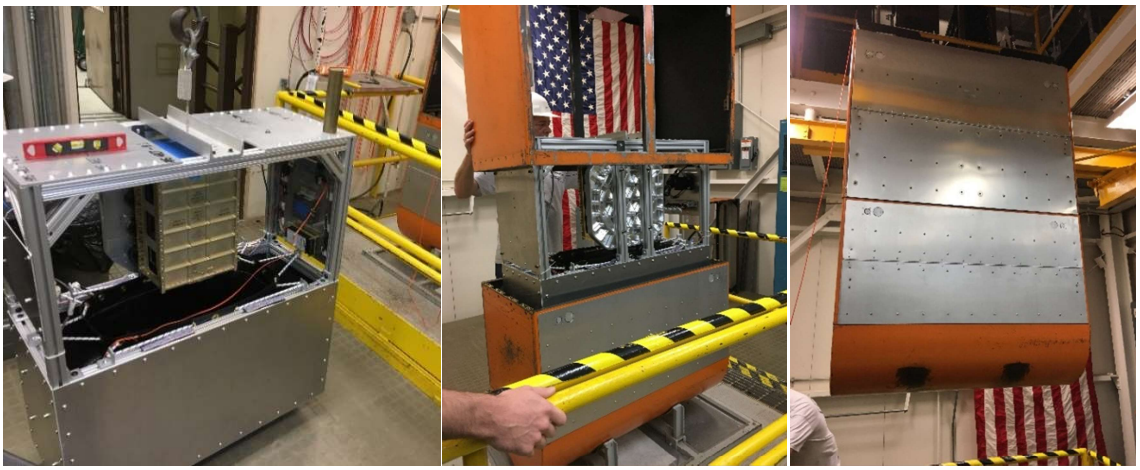

Figures 40, 41, 42. Hoisting Experiment Chassis (left), Encapsulating Experiment Chassis in Drag Shield (Center), Hoisting of Full Rig (right)

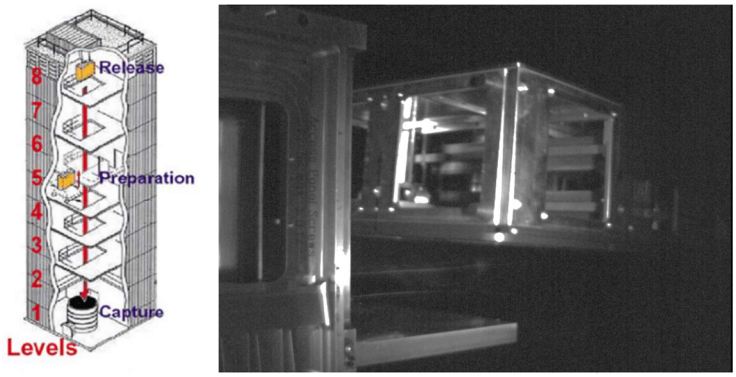

Figures 43, 44. Drop Tower Rendition *(21)* **(left), and Video Capture of Deployment (right)**

III. Results

Figure 45 through 46 shows an example of measured acceleration and angular rate data. In these plots, we show the reader how time and acceleration were measured during each experiment.

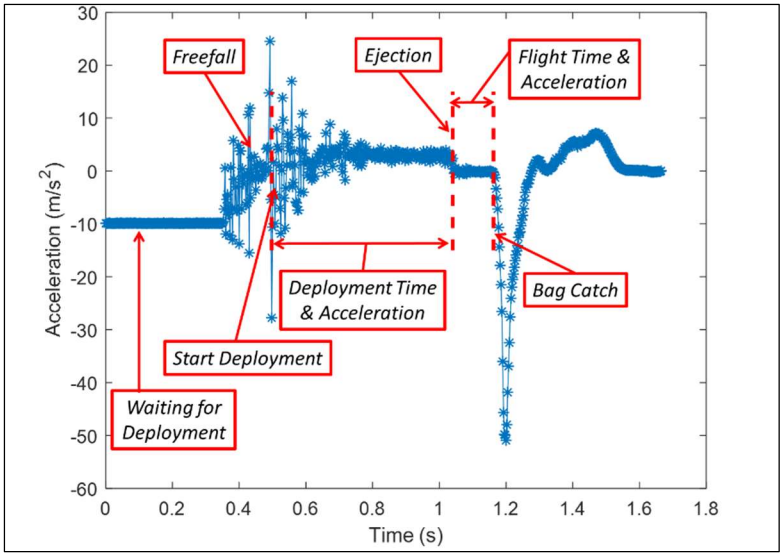

Figure 45. Identification of Linear Changes in Motion *Note the transition from -9.8 m/s² to 0 m/s². This indicates a state of freefall*

Applying the identified motion change points, it was possible to apply this to the angular motion data as well, as seen in Figure 46.

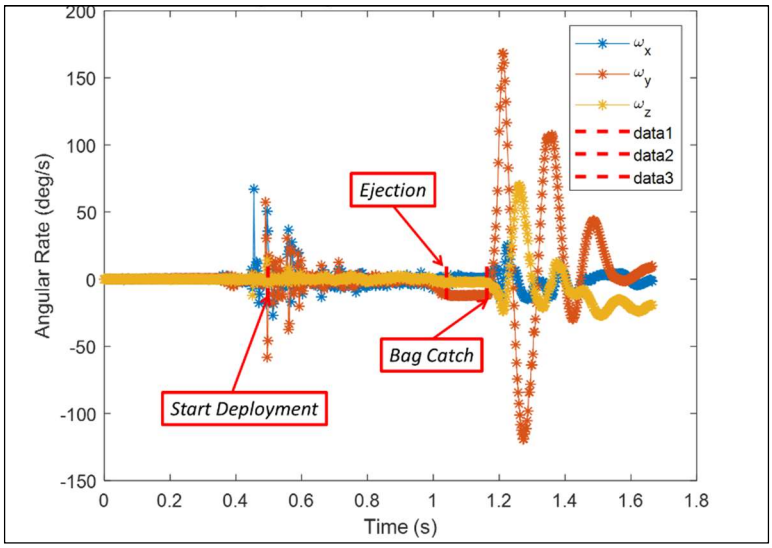

Figure 46. Angular Rate Data with Changes in Motion. *Note that the timescale corresponds with the timescale that is found in Fig. 45.*

In each of the 58 experimental data sets, the start deployment, ejection, and bag catch times had to be determine manually. MATLAB was coded to note these times, and was subsequently set to calculate average and standard deviation values of deployment and flight time, average x-axis linear acceleration and velocity (Figs. 48-50), and rotational data (Figs. 51-65). Linear and rotational motion data displayed includes the individual runs with their corresponding 1-sigma error bars (ejection velocity excludes error bars since the data point is finite, and not developed from averaging a range of values, as seen in acceleration, etc.), average standard deviation of the whole data set (taken by averaging the observed individual run standard deviations), overall observed mean (averaging individual run means), and finally the 95% two-tailed confidence interval (CI) using the average standard deviation sample (s), whole data set size (n), and the overall observed mean ($\bar{x}$). The *t*-Statistic ($t_{\alpha/2}$) is determined by n and the level of significance for a 95% CI, α=0.05. For reference, the confidence interval was calculated via Student's *t*-Statistic, as described in Eq. 1.

$$Confidence\ Interval = \bar{x} \pm t_{\alpha/2} \frac{s}{\sqrt{n}} \tag{1}$$

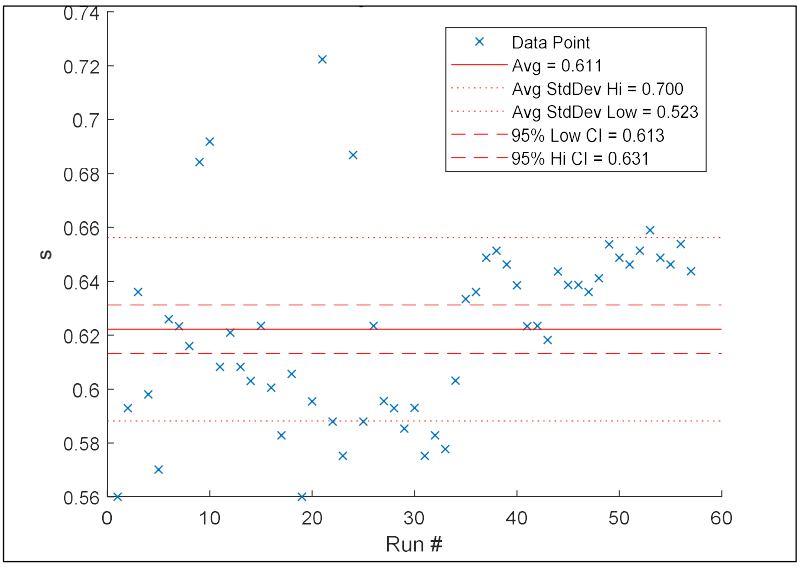

Figure 47. Deployment Time per Run

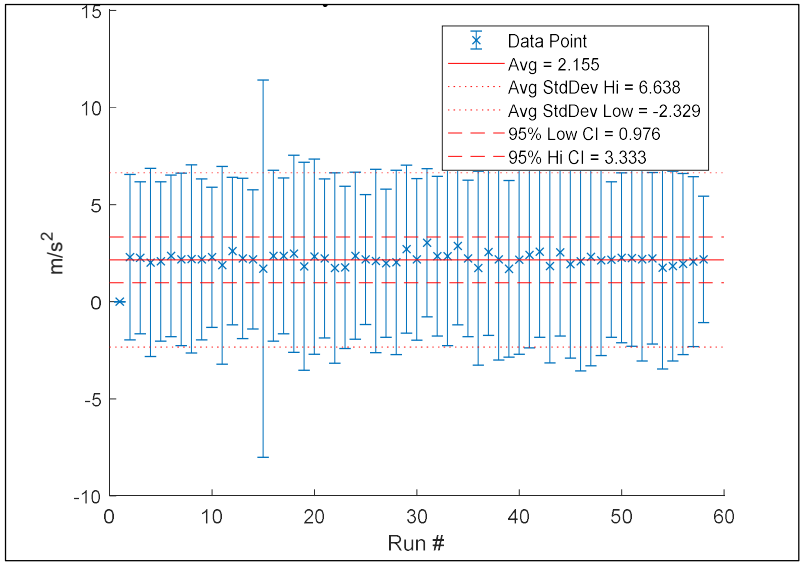

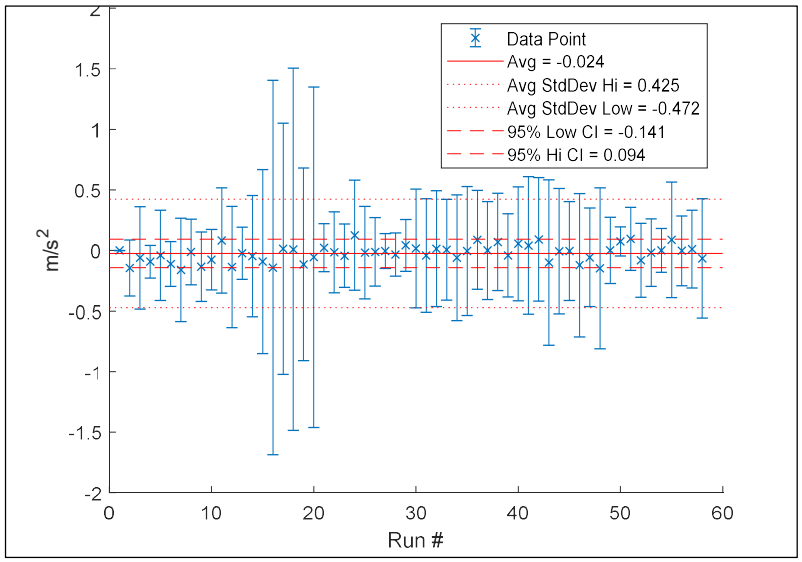

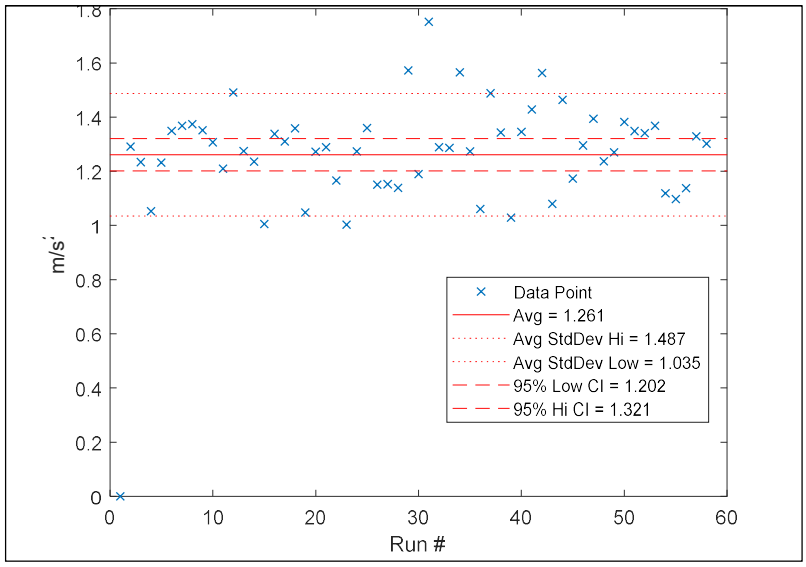

Figures 48, 49, 50. Ejection Accelerations (top) and Flight Accelerations (center), and Final Ejection Velocities (bottom) for all Experiments

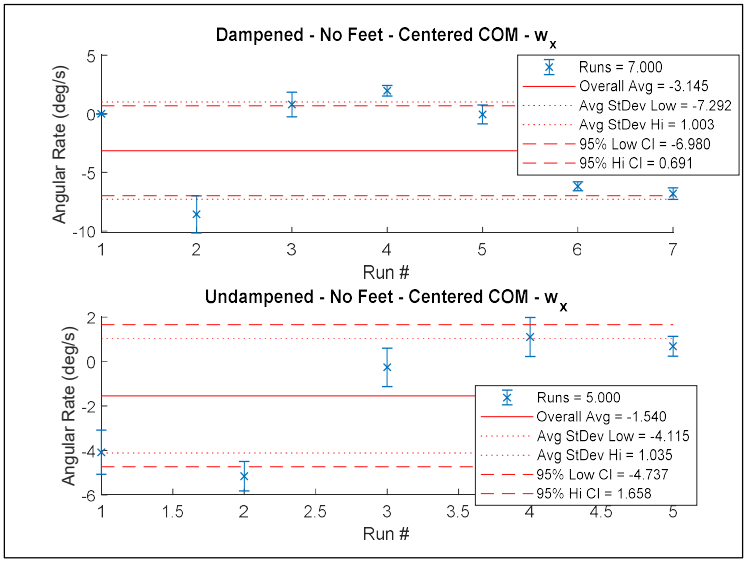

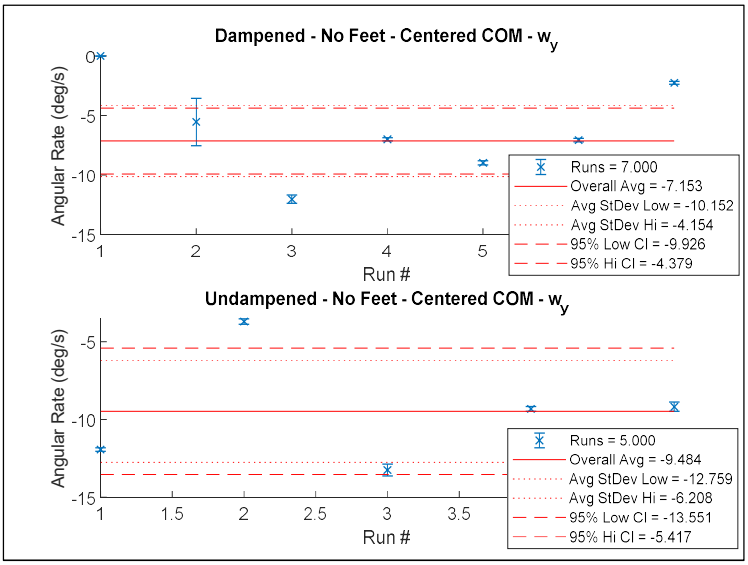

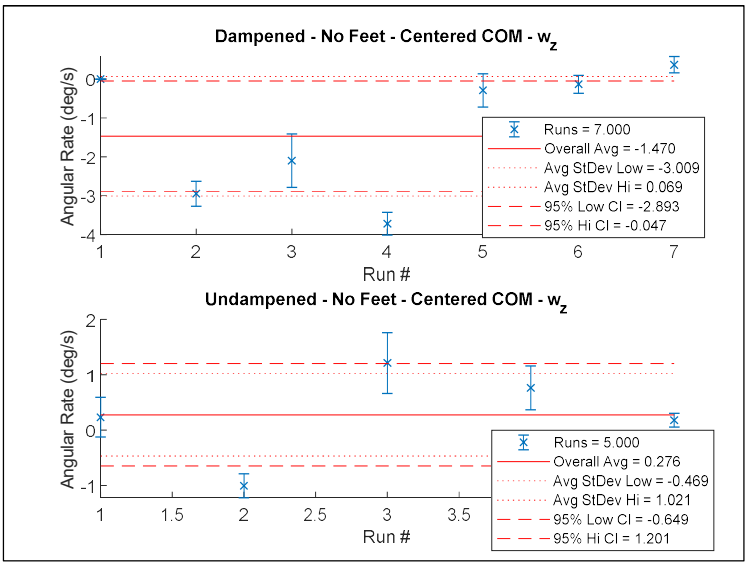

Figures 51, 52, 53. Ejection Tipoff Rates for No Feet – Centered COM Scenarios

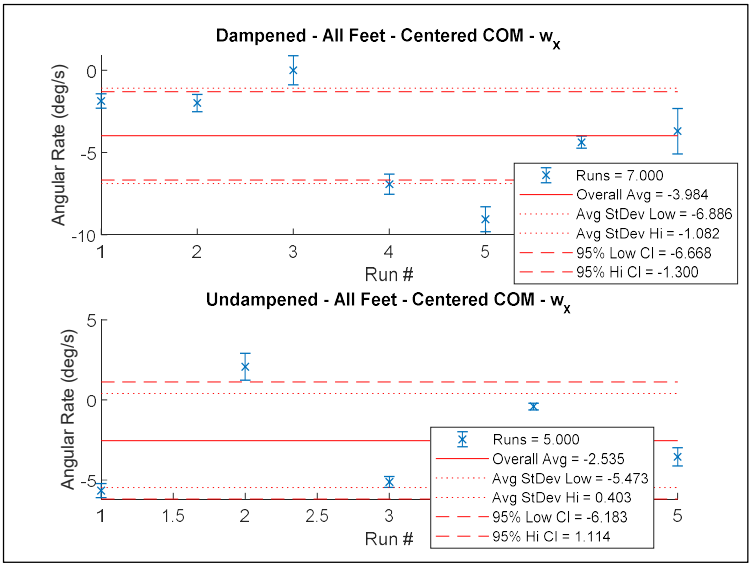

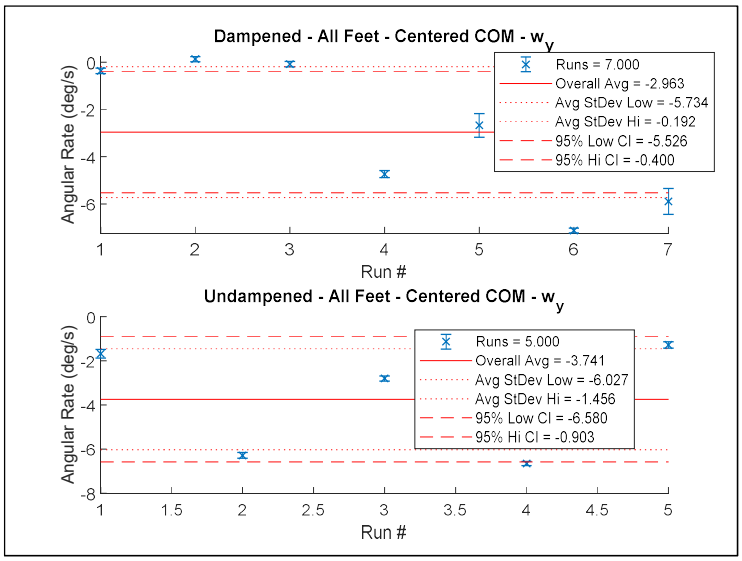

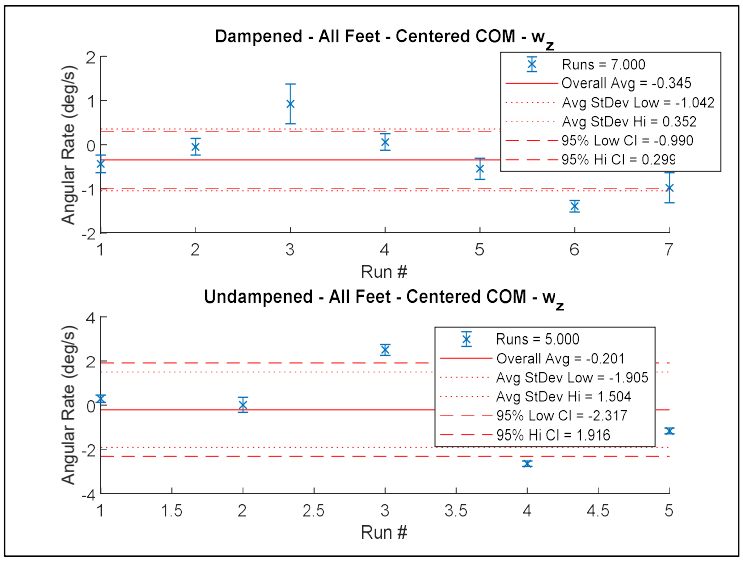

Figures 54, 55, 56. Ejection Tipoff Rates for All (Four) Feet – Centered COM Scenarios

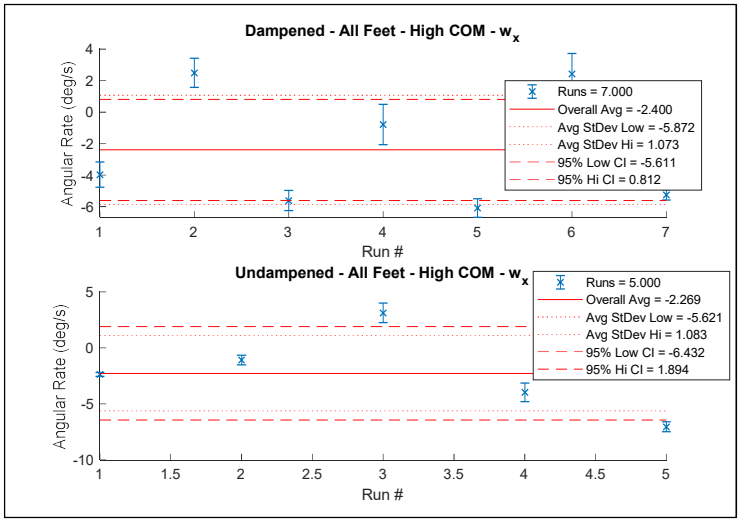

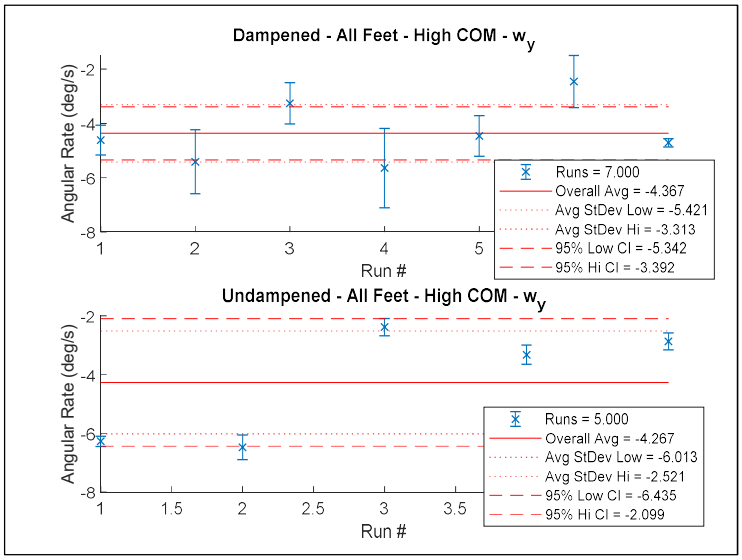

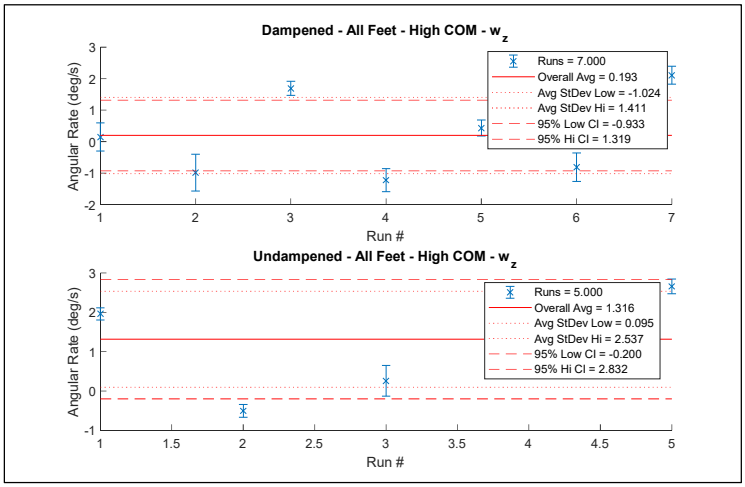

Figures 57, 58, 59. Ejection Tipoff Rates for All (Four) Feet – High COM Scenarios

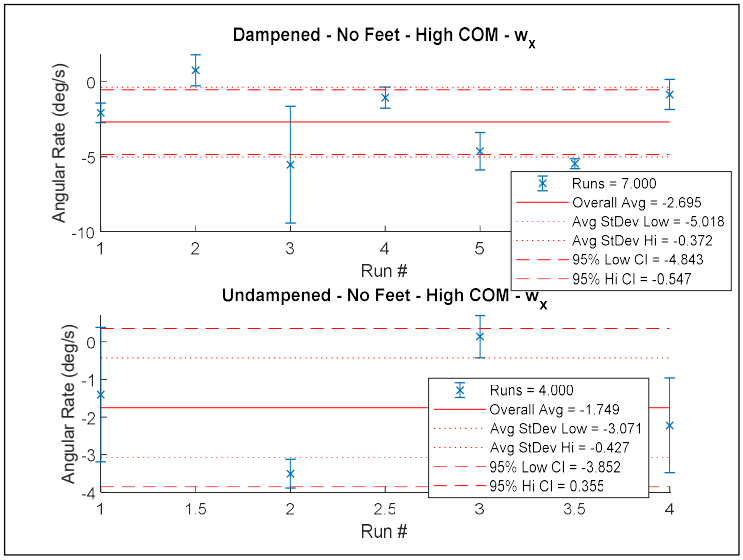

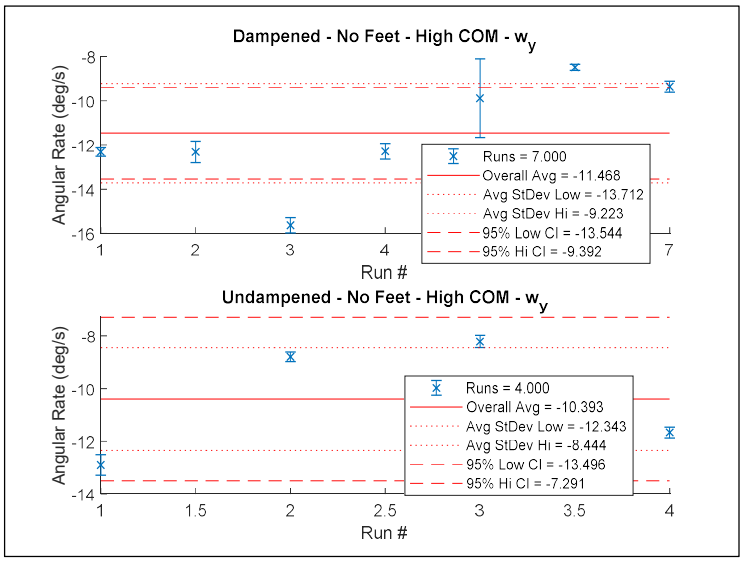

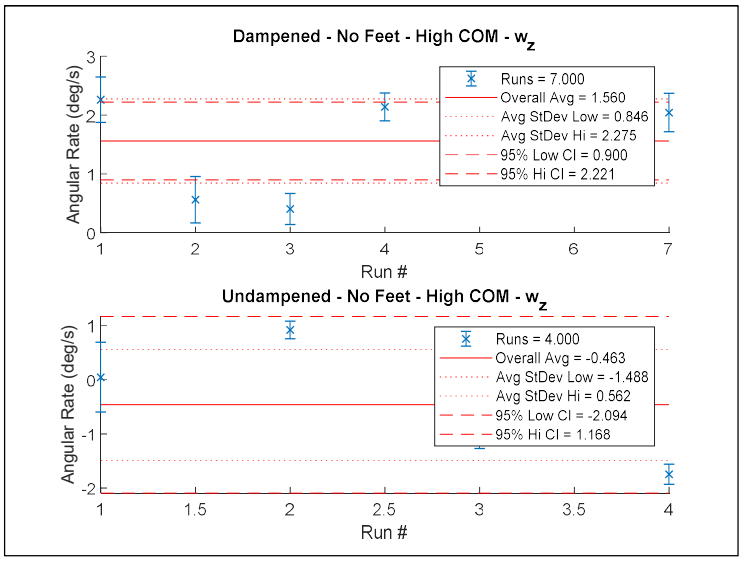

Figures 60, 61, 62. Ejection Tipoff Rates for No Feet – High COM Scenarios

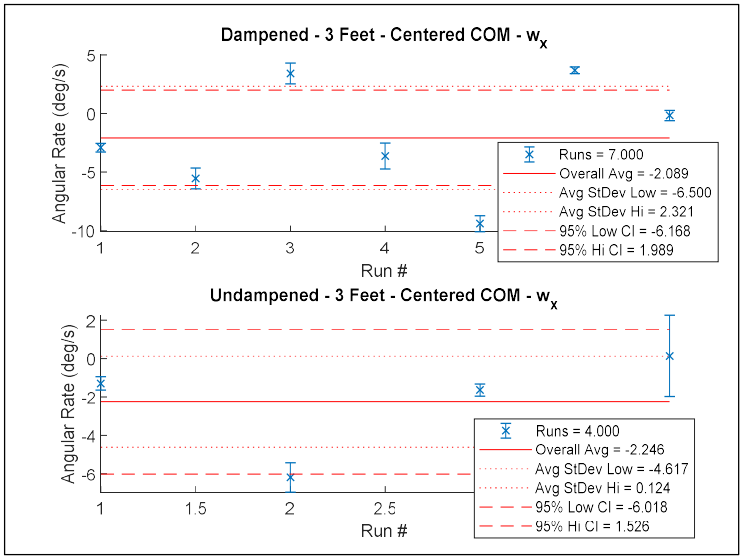

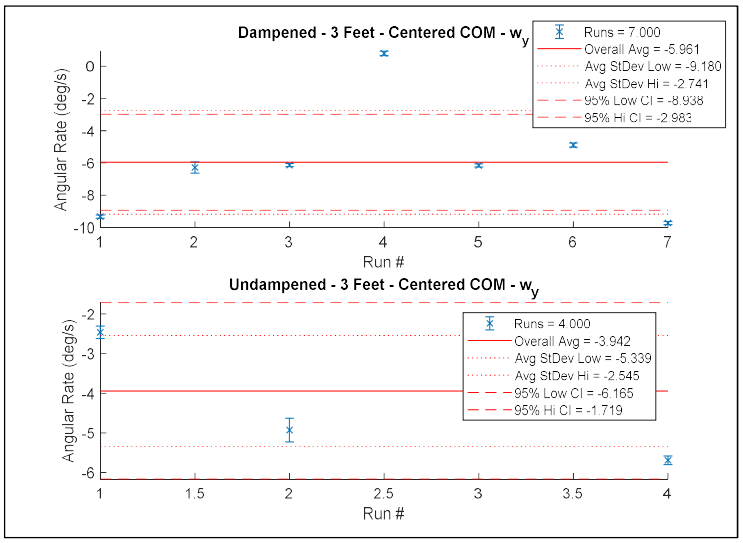

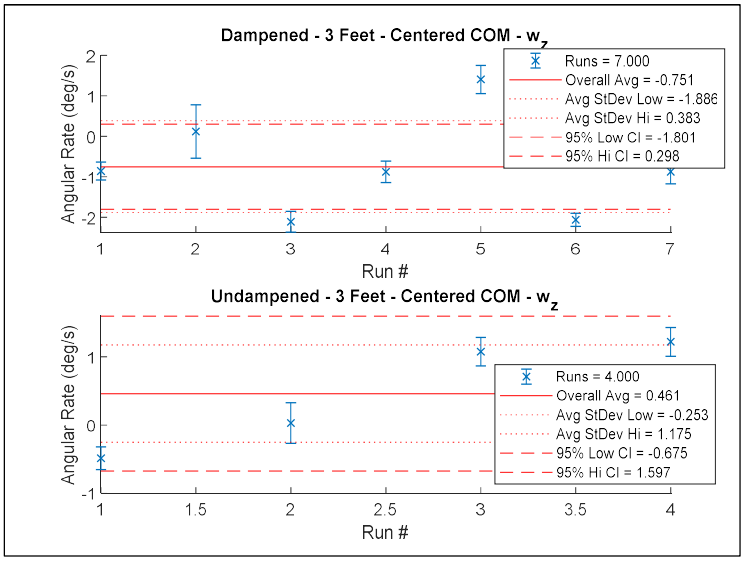

Figures 63, 64, 65. Ejection Tipoff Rates for All Feet – High COM Scenarios

One thing one notices is that for angular rates, the calculated average standard deviations of the data sets are typically quite close to the 95% confidence interval values. This gives a stronger confidence in the prediction area to where one would expect rates to fall into. The ejection and flight acceleration values were pooled together because the payloads were similar in mass, as discussed earlier. Analyzing the data validated a consistent acceleration profile (Fig. 48) for all 58 runs (average of 2.155 m/s^2, with a CI of 0.976 m/s^2 to 3.333 m/s^2), which validates the constant force nature of the CSD spring system. The flight acceleration (Fig. 49) was also consistent overall (average of -0.024 m/s^2, with a CI of -0.141 m/s^2 to 0.094 m/s^2), showing that the CubeSat stopped accelerating and was indeed in free flight. Each individual acceleration data point is plotted with error bars, because each "individual" acceleration data point was actually an averaging across the time it was accelerating. This is seen in Figure 45. The acceleration data from the IMU was integrated to yield a final ejection velocity of 1.261 m/s, with a CI of 1.202 m/s^2 to 1.321 m/s^2. This is very close to PSC' specs for a ~5.5-~5.8 kg payload (per Fig. 7), which predicts a ~1.25 m/s final ejection velocity. Considering ejection velocity results from previous research for a light 0.7 kg payload and now this data for a mid-level mass payload (mid-level because 6U two-spring CSD's have a max payload mass of 12 kg) strengthens the confidence in the CSD linear velocity profile that was originally developed from the C-9 data.

With respect to angular rates, the magnitude of the nominal centered COM-all feet configuration resulted in smaller values than what was seen on PSC's C-9 experiments. Found in Figs. 60-62, the highest overall average rate seen was -4.0 °/s, with a CI of -6.7 °/s to -1.3 °/s. The all-feet, high COM scenario (Figs. 51-53) aimed to evaluate the consequences of having a non-centered COM. This case of an offset COM resulted in higher rotation rates, as expected on the Y axis at -4.4 °/s, with a CI of -5.3 °/s to -3.4 °/s. Referring to the coordinate system in Fig. 19, a higher COM would induce a higher (negative – upward) moment during tip-off, so these values confirm that fact. For the no feet (i.e. the push plate only contacting the two bottom tabs)-centered COM configuration, the highest angular rate should be seen on the Y axis, and this was confirmed in Figs. 51-53, with an overall average rate of -7.6°/s, with a CI of -10.3°/s to -4.8°/s. To make things more interesting, the no feet, high-COM configuration saw an even higher average overall angular rate of -11.5°/s, with a CI of -13.5°/s to -9.4°/s. We see from both no-tab configurations that angular rates are significantly higher along the Y axis, but smaller along the other axes. However, the rates seen on the X and Z axes are comparable to what was seen in the nominal configuration, so the impression is that this simplified configuration may potentially complicate things for the payload, unless they're accepting the risk of higher rotation rates for the sake of simplicity. Finally, for the three-foot contact scenarios (Figs. 63-65), angular rates were higher than the all-feet configuration, where the highest average overall rate was seen at -6.0 °/s, with a CI of -8.9 °/s to -3.0 °/s. The all-feet configuration did see higher rates on the second-highest rates (on the X axis) with -4.0°/s, with a CI of –6.7 °/s to -1.3 °/s, while the three-feet configuration resulted in (on the same axis, in fact) with -2.1°/s, with a CI of –6.0°/s to -1.5°/s.

Regarding the dampened versus undampened configurations, it was noticed 12 out of 15 times in the previous figures that undampened system angular rates were smaller than the angular rates from dampened systems by an average of 1.12 °/s (standard deviation 0.75 °/s) by up to ~2.3 °/s. It is good to note that on average, the dampened configurations were run seven times, while the undampened were typically run five times due to time constraints (the dampened system was tested first).

IV. Next Steps

Future research will use this data to refine the model previously created by S. Tullino and E. Swenson. With this data, the model will be able to be more useful to mission planners, especially for our DOD and NASA partners. Also, as more mission partners are embracing the 12U construct to suit their needs, the primary author has personally received multiple requests in exploring the feasibility of duplicating this test with the 12U CSD. It would also be beneficial to replicate this test with a 6U, four-spring CSD, as this is the model of CSD used on EM-1.

V. Conclusion

As use of CubeSats increase in the space community increases, Planetary Systems Corp (PSC) will logically have more potential customers. The fact that PSC is supplying deployers for the high-visibility Space Launch System (SLS) Exploration Mission 1 (EM-1) will likely yield a boost in Canisterized Satellite Dispenser (CSD) interest. Moreover, mainstream CubeSat chassis manufacturers such as Pumpkin and Blue Canyon Technologies favoring the CSD medium will increase potential customers, thus driving the need for a better understanding of deployment rates will

emerge. These microgravity deployment tests conducted at NASA Glenn Research Center's (GRC's) drop towers bridged data gaps that PSC encountered during their C-9 tests. Specifically, the drop tower did not suffer from induced rotations from the C-9. Data knowledge from these tests have narrowed the confidence interval in the CSD's capabilities, which overall is highly beneficial to PSC and its customers. When using PSC spec, expected angular rates have been demonstrated to be on average lower than what the original <10 °/s envelope was. The widths in the angular rate confidence intervals and standard deviations do warrant the question of what is causing angular rate variation. The primary suspect causing this is the flexion in the CSD push plate. This is possible because a person can flex the plate easily with his own hand. Future research on the push plate should focus on the degree of flexion, and how the plate can be stiffened, while maintaining a light mass. Moreover, an intermediate mass (~5-6 kg) for the two-spring 6U CSD validated PSC's linear velocity curve even more. (S. Tullino's thesis already validated linear velocities for the light mass end (<1 kg).) Also demonstrated were the effects of deviating from PSC spec: specifically having a COM outside of the recommended geometric envelope, or not having the recommended contact points enveloping the COM. It was also discovered how the Moog Isolators seemed to have impacted angular rates: not by much, but still notable to discuss for possible future research. PSC and the SLS EM-1 secondary payload team has requested having data like this be available to ensure mission success via the more precise characterization of the CSD. Ultimately, this data will enable the tuning of the MATLAB CSD deployment simulation model that can be available to payload planners to assist in payload design and mission planning.

Acknowledgments

The primary author would like to thank Dr. Eric Swenson (the primary author's thesis advisor while AFIT) for all his ceaseless interest, assistance with this research, data analysis, and encouragement even after the primary author graduated. The primary author would also like to thank his wife, Jessica Tullino for her assistance in data analysis, literature review, and data presentation. A special thanks to Walter Holemans from PSC for his support, motivation, openness, and validation of this project. In addition, a special thanks to Randall Sharp, Phillip Smith, Sean Miller, Christopher Sheffield, and Jorge Urena for help with designing, building, and consultation for all apparatuses needed for this research. Thanks to Joe Battigaglia of Battigaglia's Upholstering, who helped finalize the design and created test rig catcher bag design. Another thanks to Eric Neumann, Luke Ogorzaly, Dan XXX, and XXX from NASA GRC for their assistance with the drop towers. Moreover, thanks to John Howat and Timothy Pargett from Moog in lending the experiment their isolators. A special thanks to Scott Spearing from NASA Marshall Space Flight Center, who provided project concept validation and helped facilitate discussion of this project with the Space Launch System Secondary Payloads team. The author also appreciates the NASA team who provided project consultation and vetting: Joseph Pelfrey from NASA Marshall, Bruce Yost and Elwood Agasid from NASA Ames Research Center, Scott Higginbotham from NASA Kennedy Space Center, and Dr. Jitendra Joshi, Technology Integration Lead for the Advanced Exploration Systems Division at NASA Headquarters for providing vetting and for his considering funding for this project. A special thanks to Lt Col Christopher Allen from AFRL Space Vehicles Directorate for facilitating the funding of this project.

References

1. **Holemans, Walter and Henver, Ryan.** *Canisterized Satellite Dispenser. US 2014/0319283 A1* United States of America, October 30, 2014. Patent Application Publicatoin.
2. **Henver, Ryan.** Canisterized Satellite Dispenser (CSD) Data Sheet (2002337D). [Online] Planetary Systems Corporation, August 4, 2016. http://www.planetarysystemscorp.com/web/wp-content/uploads/2016/08/2002337D-CSD-Data-Sheet.pdf.
3. *Lessons Learned Testing and Flying Canisterized Satellite Dispensers (CSD) for Space Science Missions.* **Azure, Floyd, et al.** Palo Alto, CA : 3rd Annual Lunar Cubes Workshop, 13-15 November 2013.
4. **Pumpkin Space Systems.** 6U SUPERNOVA Structure Kit Owner's Manual. [Online] 2014. http://www.cubesatkit.com/docs/SUPERNOVA_User_Manual-RevA0.pdf.
5. **Azure, Floyd, Hevner, Ryan and Holemans, Walter.** *Lessons Learned Measuring 3U and 6U Payload Rotation and Velocity when Dispensed in Reduced Gravity Environment.* 21 April 2015.
6. **Holemans, Walter and Flood, Christopher.** *Interview with PSC on CSD Deployment Profiles.* July 28, 2016.
7. **Henver, Ryan.** Payload Specification for 3U, 6U, 12U and 27U. [Online] Planetary Systems Corporation, August 4, 2016. http://www.planetarysystemscorp.com/web/wp-content/uploads/2016/08/2002367D-Payload-Spec-for-3U-6U-12U-27U.pdf.
8. **Pumpkin Inc.** Picture of CSD Push Plate after SUPERNOVA Vibe Test. Wright-Patterson AFB : s.n., 2016.
9. **Spearing, Scott.** *NASA Marshall SLS Secondary Payload Program Consultation.* November 14, 2016.
10. **Pumpkin Inc.** Picture of SUPERNOVA CubeSat CSD Contact Feet. Wright-Patterson AFB : AFIT, 2016.
11. **Spearing, Scott.** *Discussion at 2018 AIAA/USU SmallSat Conference.* Logan, August 8, 2018.
12. **Elonen-Wright, Linda C.** NASA GRC Zero Gravity Research Facility. *NASA Glenn Research Center.* [Online] January 24, 2008. [Cited: September 19, 2016.] http://facilities.grc.nasa.gov/zerog/.
13. **Neumann, Eric.** *NASA GRC Zero-G Facility Consultation.* October 2016.
14. **Gotti, Daniel J.** A Collection of 2.2 Second Drop Tower Information. Cleveland, Ohio : NASA Glenn Research Center - National Center for Space Exporation Research, October 2005.
15. **X-io Technologies.** Next Generation IMU User's Manual. 2016.
16. *Testing and Evaluating Deployment Profiles of the Canisterized Satellite Dispenser (CSD).* **Tullino, Stephen K.** Grapevine : 55th AIAA Aerospace Sciences Meeting, AIAA SciTech Forum, 2017. AIAA 2017-0850.
17. **Tullino, Stephen K.** *Testing and Evaluating Deployment Profiles of the Canisterized Satellite Dispenser (CSD).* Wright-Patterson AFB, OH : Air Force Institute of Technology, 2017.
18. **Moog CSA Engineering.** CubeSat Installation 1. *CAD Drawing.* Mountain View : Moog CSA Engineering, 2017. Cage Code: 8V815.
19. **Del Rosso, Dominic.** Reduced Gravity Research. *NASA/JSC Aircraft Operations.* [Online] September 30, 2016. https://jsc-aircraft-ops.jsc.nasa.gov/Reduced_Gravity/index.html.
20. **Sharp, Randall.** Drop Tower Inner Chassis Design Consult. Wright-Patterson AFB : s.n., 2016.
21. **Elonen-Wright, Linda C.** NASA GRC 2.2 Second Drop Tower. *NASA Glenn Research Center.* [Online] National Aeronautics and Space Administration, February 1, 2008. [Cited: September 19, 2016.] http://facilities.grc.nasa.gov/drop/.
22. **Swenson, Eric.** *MECH 632 Intermediate Spaceflight Dynamics & Thesis Advisor.* April - September 2016.
23. **Henver, Ryan.** 3000257B CSD Operating and Integration Procedure. s.l. : Planetary Systems Corp, 2016.